PHILOSOPHICAL TRANSACTIONS OF THE ROYAL SOCIETY A MATHEMATICAL, PHYSICAL & ENGINEERING SCIENCES

Flame Stretch Rate as a Determinant of Turbulent Burning Velocity

D. Bradley, A. K. C. Lau and M. Lawes

Phil. Trans. R. Soc. Lond. A 1992 **338**, 359-387
doi: 10.1098/rsta.1992.0012

Flame stretch rate as a determinant of turbulent burning velocity

By D. Bradley, A. K. C. Lau and M. Lawes

Department of Mechanical Engineering, University of Leeds, Leeds LS2 9JT, U.K.

Contents

A rational basis for correlating turbulent burning velocities is shown to involve the product of the Karlovitz stretch factor and the Lewis number. A generalized expression is derived to show how flame stretch is related to the velocity field. A new dimensionless correlation of experimental values of turbulent burning velocities is presented. Dimensionless groups also are used in correlations of laminar and turbulent flame extinction stretch rates. A distribution function of stretch rates in turbulent flames, based on an earlier one of Yeung *et al.*, is proposed and the experimental data are well predicted by a theory based on flamelet extinction by flame stretch with this distribution. Uncertainties arise concerning the role of negative stretch rate. Laminar flamelet modelling of complex combustion appears to have a broader validity than might be expected and some explanation for this is offered.

0. Nomenclature

A constant; in equation (1)

A elemental area of the flame surface

A_r fraction of the mean flame front area supporting propagation, equation (33)

a stretch dependency factor, also stretch rate on a material surface normalized by the Kolmogorov time

c value of u_t/u_l from curve, figure 4, equation (13)

Phil. Trans. R. Soc. Lond. A (1992) **338**, 359–387
Printed in Great Britain

e	experimental value of u_t/u_l, equation (13)
K	dimensionless Karlovitz stretch factor
$\mathscr{K}$	dimensionless stretch rate
$\bar{\mathscr{K}}$	dimensionless mean stretch rate
$\mathscr{K}_q$	dimensionless laminar quench stretch rate
$\mathscr{K}_{qt}$	dimensionless turbulent quench stretch rate
L	integral length scale of turbulence
Le	Lewis number
$L_{i\alpha}$	transformation matrix
Ma	Markstein number
n_i	unit normal vector in cartesian coordinates
N_i	unit normal vector in general coordinates
$\boldsymbol{n}$	unit vector normal to the flame front
$p(s)$	PDF of s
$p(\theta)$	PDF of θ
$p(\theta, s)$	joint PDF of θ and s
$\tilde{q}_t$	mean, mass weighted, turbulent, volumetric heat release rate
R	radius of curvature
R_L	turbulent Reynolds number $(= u'L/\nu)$
R_λ	turbulent Reynolds number $(= u'\lambda/\nu)$
s	stretch rate
$\bar{s}$	mean stretch rate
s_{ij}	strain rate tensor
s_q	quenching stretch rate
s_{qt}	turbulent quenching stretch rate
T	gas temperature
T_b	burnt gas temperature
T_u	unburnt gas temperature
u'	r.m.s. turbulent velocity
u'_k	effective r.m.s. turbulent velocity acting on a flame
U_i	surface velocity component in general coordinate system
u_i	cartesian velocity component
u_l	laminar burning velocity
u_n	stretched laminar burning velocity
u_t	turbulent burning velocity
u_{to}	unstretched turbulent burning velocity
V_i	fluid velocity component in general coordinate system
x	dummy variable of integration
x_i	cartesian coordinate
X_i	general coordinate
α	stretch rate on a random surface normalized by the Kolmogorov time
β	Zeldovich number
γ	expansion ratio
δ_l	laminar flame thickness
ϵ	turbulent dissipation rate
ϵ_f	upper limit of ϵ acting on a flame
η	Kolmogorov length scale of turbulence
θ	reaction progress variable, also polar coordinate
$\tilde{\theta}$	Favre mean of θ
$\tilde{\theta}''^2$	Favre mean of variance of θ
λ	Taylor microscale of turbulence
ν	kinematic viscosity
ρ_b	burnt gas density
ρ_u	unburnt gas density
σ	standard deviation
σ_s	r.m.s. rate of stretch
$\sigma_{\mathscr{K}}$	dimensionless r.m.s. rate of stretch
τ_f	effective dissipative timescale acting on a flame
τ_η	Kolmogorov timescale of turbulence
ϕ	equivalence ratio, also polar coordinate
$\nabla_t \boldsymbol{u}$	surface velocity gradient

1. Introduction

A correlation of all known measurements, about 1650 in number, of turbulent burning velocity, u_t, in the absence of strong pressure fields and macro-vorticity, has

PHILOSOPHICAL TRANSACTIONS OF THE ROYAL SOCIETY A MATHEMATICAL, PHYSICAL & ENGINEERING SCIENCES

been presented previously in terms of the ratios of turbulent to unstretched laminar burning velocity, u_t/u_l, effective cold premixture r.m.s. turbulent velocity acting on the flame to laminar burning velocity, u'_k/u_l, and Karlovitz flame stretch factor, K (Abdel-Gayed *et al.* 1987). For flames propagating from a point source, the value of u'_k is related by an algebraic expression to the r.m.s. turbulent velocity, u', in terms of a dimensionless elapsed time. This is the elapsed time normalized by the turbulence autocorrelation time. In turbulent flow the dimensionless Karlovitz stretch factor is the eulerian mean strain rate of the premixture, u'/λ, normalized by a laminar flame 'chemical' strain rate given by u_l/δ_l. Here λ is the Taylor microscale of turbulence and δ_l is the laminar flame thickness, usually approximated by ν/u_l, where ν is the kinematic viscosity of the premixture. This is the thermal thickness, a reaction zone thickness can be derived from it and the activation energy of the reaction (Sivashinsky 1990). Alternatively, K can be interpreted as a ratio of chemical to eddy lifetimes.

For isotropic turbulence, with λ related to the integral length, L, by

$$\lambda^2/L = A\nu/u' \tag{1}$$

and with a value of A equal to 40.4, it easily can be shown (Abdel-Gayed *et al.* 1984) that

$$K = 0.157(u'/u_l)^2 R_L^{-0.5}. \tag{2}$$

Here R_L is the turbulent Reynolds number, $u'L/\nu$, and it is through this parameter that the influence of length scale is expressed. There is also an influence of the Lewis number of the premixture, Le, given by the thermal diffusivity divided by the diffusion coefficient of the deficient reactant. Separate correlations were presented for $Le \leqslant 1.3$ and $Le > 1.3$.

The correlations embrace many fuels and mixture strengths, but because problems of measuring accurately are compounded with those of seeking an overall generalization, it is not surprising that there is appreciable scatter in the values of the dimensionless groups. Nevertheless, the correlation has proved useful in, for example, such apparently diverse problems as the estimations of combustion rates in gasoline engines (Bradley *et al.* 1988*b*), of overpressures in unconfined atmospheric explosions (Abdel-Gayed & Bradley 1982) and of flame propagation rates in fine dust mixtures (Bradley *et al.* 1989*a*).

Most theories of turbulent combustion invoke the laminar flamelet assumption, namely, that the molecular rates of transport and of chemical reaction predominate over the rates of turbulent fluctuations. Some laminar flamelet concepts have been reviewed by Peters (1988). Essentially, the localized flame structure is that of a laminar flame and a turbulent flame is an array of laminar flames. A starting point in classical analyses of laminar flames is to assume that the flow is one dimensional, that the reaction is bimolecular and Le is unity. The consequent equality between the flux of energy due to diffusion of fuel molecules and the equal and opposite flux due to conduction leads to a constant enthalpy flame. When Le departs from unity this balance is destroyed and if, in addition, the flow diverges there is further unbalance due to an additional convective flux along the flame surface. When a flame is stretched in this way the balance between these fluxes is so changed that ultimately the flame may be quenched (Karlovitz *et al.* 1951; Tsuji & Yamaoka 1981; Law *et al.* 1988). This has been observed to occur also with turbulent flames (Abdel-Gayed & Bradley 1985), although a statistical definition of quench was required.

High-speed schlieren photography of a variety of turbulent explosion flames

PHILOSOPHICAL TRANSACTIONS OF THE ROYAL SOCIETY A MATHEMATICAL, PHYSICAL & ENGINEERING SCIENCES

reveals different combustion régimes. In sequential order of increasing flame stretch these comprise first the continuous flame sheet, to be followed by partial and, eventually, complete quenching, all correlated by the product KLe (Abdel-Gayed *et al.* 1989*b*). When KLe attains a value of about 0.15, the continuous flame sheet begins to break up, a process which is accelerated by increasing flame quenching at values of KLe greater than 0.3. It is not infrequently assumed in turbulent combustion that a wrinkled laminar flame structure requires that the laminar flame thickness, δ_l, must be smaller than the Kolmogorov microscale, η (Williams 1976). Another cited criterion, which essentially is identical, is that the chemical time, δ_l/u_l, must be smaller than the Kolmogorov time, τ_η. Both conditions lead to $K < 0.258$ (Abdel-Gayed *et al.* 1989*b*).

There are two principal, and opposing, influences of turbulence upon the turbulent burning velocity. The turbulent wrinkling of the flame front increases the flame area and hence u_t. Andrews *et al.* (1975) summarize many wrinkled laminar flame models, most of which, since the seminal work of Damköhler (1940), have expressed u_t/u_l as a function of u'/u_l, sometimes with a linear increase of u_t with u'. This is supported by the more recent theoretical work of Clavin (1988). The opposing influence is that of flame stretch, which reduces u_t. The result is that with a given system and premixture, as the turbulence increases, initially the flame wrinkling effect predominates to be followed later by partial quenching due to flame stretch. As a consequence, the value of u_t first increases, then finally decreases before complete extinction. Activation energy asymptotic analyses of wrinkled laminar flames by Clavin & Williams (1979, 1981, 1982) show that to second order in the ratio δ_l/L the effect on burning velocity involves only the mean area increase due to wrinkling, but that to fourth order mean stretch and curvature effects become important, and these depend upon the value of Le.

A theoretical consideration of flame stretch and associated velocity field in §2 shows the important influence of the product KLe. First laminar flames are considered. Turbulent flames are more complex because of uncertainties about both the distribution of stretch rates on the flamelets (Abdel-Gayed *et al.* 1989*a*; Yeung *et al.* 1990), and the validity of the laminar flamelet assumption (Bilger 1989). The concept of an extinction flame stretch rate has proved to be useful in both experimental (Law 1988) and computational (Dixon-Lewis 1988*a*, *b*; Stahl *et al.* 1988) studies of laminar flames and values of this parameter have been found. These are applied to turbulent flames in §4, in conjunction with a probability density function (PDF) of the stretch rate that is similar to that proposed by Yeung *et al.* (1990). This yields a correlation of turbulent burning velocities that compares well with the experimental correlations. A further modification of this distribution law gives even better agreement between flamelet predictions of u_t/u_l and the experimental values. This is an important conclusion for the mathematical modelling of turbulent combustion.

2. Flame stretch

The change in laminar burning velocity to a value of u_n, as a consequence of flame stretch, $A^{-1}(\mathrm{d}A/\mathrm{d}t)$, can be expressed by (Clavin 1985, 1988):

$$\frac{u_l - u_n}{u_l} = \frac{1}{A}\frac{\mathrm{d}A}{\mathrm{d}t}\frac{\delta_l}{u_l}Ma. \tag{3}$$

Here A is an infinitesimal area of the flame surface, t is time and Ma the Markstein number, the ratio of the Markstein length to δ_l. This length originally arose phenomenologically to express stretch and curvature effects (Markstein 1964). It also has an influence on flame stability.

With A as the area of a material surface, Batchelor (1967) has derived a general expression in cartesian coordinates for its stretch rate in terms of the flow field:

$$\frac{1}{A}\frac{\mathrm{d}A}{\mathrm{d}t} = \frac{\partial u_j}{\partial x_j} - n_i n_j \frac{\partial u_i}{\partial x_j} = (\delta_{ij} - n_i n_j)\frac{\partial u_i}{\partial x_j}. \tag{4}$$

Here u_i, δ_{ij} and n_i are the tensor components of fluid velocity, the delta function and unit normal vector of the material surface, respectively. This expression is also applicable to any specified surface for which u_i is the velocity.

Since $A^{-1}(\mathrm{d}A/\mathrm{d}t)$ is a scalar quantity, (4) is frame invariant and this cartesian expression may be transformed into one for any set of general curvilinear coordinates by the substitutions:

$$\delta_{ij} = L_{i\alpha}L_{j\beta}\delta_{\alpha\beta}, n_i = L_{i\alpha}N_\alpha, u_i = L_{i\alpha}U_\alpha, \partial/\partial x_j = L_{j\beta}\partial/\partial X_\beta, \tag{5}$$

where $L_{i\alpha}$ is the transformation matrix between the cartesian and the new coordinates and $\delta_{\alpha\beta}, N_\alpha, U_\alpha$ and X_α are the corresponding tensor quantities of δ_{ij}, n_i, u_i and x_i. Substitution of (5) into (4) gives

$$\frac{1}{A}\frac{\mathrm{d}A}{\mathrm{d}t} = (\delta_{\alpha\beta} - N_\alpha N_\beta)\left(\frac{\partial U_\alpha}{\partial X_\beta} + L_{j\alpha}\frac{\partial L_{j\sigma}}{\partial X_\beta}U_\sigma\right). \tag{6}$$

This expresses the stretch rate in terms of the velocity of the specified surface and the surface geometry, which defines N_i and $L_{i\alpha}$. The coordinates can be defined arbitrarily and it is convenient to allow the surface to lie on the X_2X_3-plane with its normal in the X_1 direction. This convention is adopted in the present paper for all flame surfaces. Hence, the only non-zero component of the unit normal vector is $N_1 = 1$ and, when expanded, (6) becomes

$$\begin{aligned}\frac{1}{A}\frac{\mathrm{d}A}{\mathrm{d}t} = {} & \left(L_{j2}\frac{\partial L_{j1}}{\partial X_2} + L_{j3}\frac{\partial L_{j1}}{\partial X_3}\right)U_1 \\ & + \left(\frac{\partial U_2}{\partial X_2} + \left(L_{j2}\frac{\partial L_{j2}}{\partial X_2} + L_{j3}\frac{\partial L_{j2}}{\partial X_3}\right)U_2 + \frac{\partial U_3}{\partial X_3} + \left(L_{j2}\frac{\partial L_{j3}}{\partial X_2} + L_{j3}\frac{\partial L_{j3}}{\partial X_3}\right)U_3\right).\end{aligned} \tag{7}$$

This can also be written as,

$$\frac{1}{A}\frac{\mathrm{d}A}{\mathrm{d}t} = \frac{1}{R}U_1 + \nabla_{\mathrm{t}}\boldsymbol{U} = \frac{\partial u_j}{\partial x_j} - n_i n_j \frac{\partial u_i}{\partial x_j}, \tag{8}$$

in which R is the total radius of the flame curvature, defined by

$$1/R = (L_{j2}\partial L_{j1}/\partial X_2 + L_{j3}\partial L_{j1}/\partial X_3) \tag{9}$$

and $\nabla_{\mathrm{t}}\boldsymbol{U}$ denotes the velocity gradient along the surface, given by the second overall bracketed term on the right of (7).

Such generality is important for the consideration of flame stretch because of the diverse shapes that flames might assume. A surface may be defined by an isotherm or any isoscalar surface. The rate of change of area term is the flame stretch and the velocity of the flame surface normal to itself is the flame speed. This is the sum of the

burning velocity, u_n, and the fluid velocity in that direction, which here is taken to be that of the X_1 coordinate. The tangential velocities along the surface in the X_2 and X_3 directions are those of the fluid. When (5)–(9) are applied to a flame surface and the fluid velocity components are denoted by $V_\alpha = (V_1, V_2, V_3)$ it therefore follows that

$$U_1 = u_n + V_1, U_2 = V_2 \quad \text{and} \quad U_3 = V_3. \tag{10}$$

Equation (8) then expresses the flame stretch by

$$\frac{1}{A}\frac{\mathrm{d}A}{\mathrm{d}t} = \frac{u_n}{R} + \left(\frac{V_1}{R} + \nabla_t V\right). \tag{11}$$

The bracketed terms, for this coordinate system, are essentially those on the right of (4) and represent the flow field, or rate of strain tensor, contribution to flame stretch. The first term on the right of (11) represents the flame propagation and curvature contribution to flame stretch. The localized influences of curvature upon flame structure can be important. The contrast between concave and convex curvatures has been revealed by laser-induced fluorescence of OH radicals in thin sheets (Becker *et al.* 1990). However, in turbulent flames the effects of positive and negative curvatures will tend to cancel each other, the first term will become very small and the bracketed terms will predominate.

In any case, as flow and turbulent velocities increase, the bracketed terms will increase relative to the first term. Thus the main contribution to flame stretch arises from the flow field stretch ahead of the flame. This is a mean lagrangian quantity that will generally be positive and, for isotropic turbulence, proportional to the eulerian mean strain rate, u'/λ (Batchelor 1952). It follows from (3) and (11) that the average fractional reduction in burning velocity of laminar flamelets is proportional to KMa.

The Markstein number is a physicochemical parameter that expresses the response of a flame to stretching. Neither its theoretical nor its experimental evaluation are easy, although Searby & Quinard (1990) have recently presented some experimental values. The value depends in a detailed way upon chemical kinetics and the transport properties. For a two reactant mixture with a single step reaction rate the asymptotic analysis of Clavin & Williams (1982) yields

$$Ma = \frac{1}{\gamma}\ln\left(\frac{1}{1-\gamma}\right) + \tfrac{1}{2}\beta(Le-1)\frac{1-\gamma}{\gamma}\int_0^{\gamma/(1-\gamma)}\frac{\ln(1+x)}{x}\,\mathrm{d}x, \tag{12}$$

where x is a dummy variable of integration, β the Zeldovich number and γ the expansion ratio $(\rho_\mathrm{u}-\rho_\mathrm{b})/\rho_\mathrm{u}$ with ρ_u and ρ_b densities of unburned and burned gas. Because of the dearth of experimental data on Ma, it has been evaluated by Harper (1989) over a wide range of mixtures from (12) and shown to change linearly with Le. This explains the emergence of KLe as a dimensionless group that can generalize the effects of flame stretch. For the present therefore, we shall adopt the KLe, rather than the more rigorous KMa grouping, in the more generalized correlation of experimental values of u_t to be presented in §3. The values of Le are based on an assumed simplistic reaction of fuel and oxygen molecules (Abdel-Gayed *et al.* 1985).

3. Correlation of turbulent burning velocities in terms of KLe

The earlier correlation, for two different ranges of Le, (Abdel-Gayed *et al.* 1987) gave values of u_t/u_1, plotted against those of u'_k/u_1 for different values of K in two

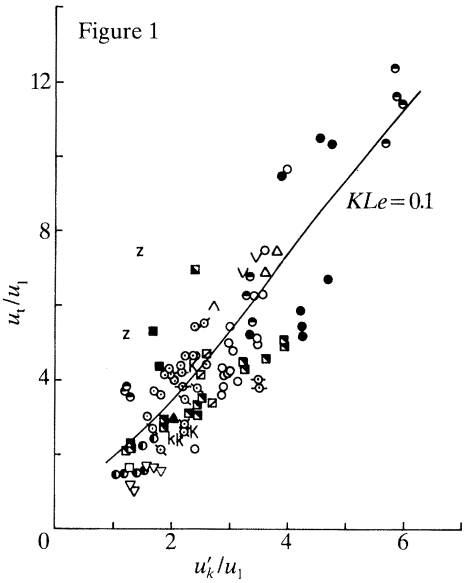

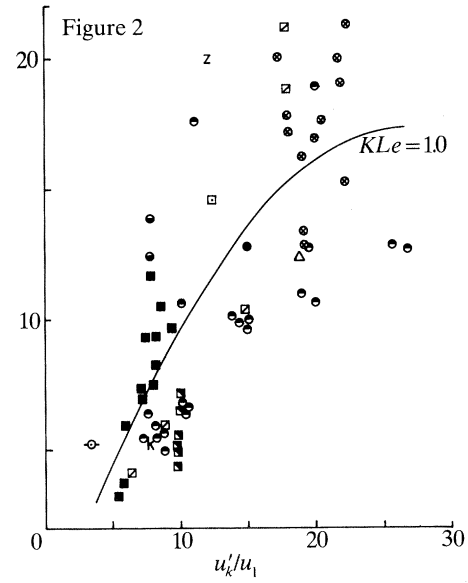

Figure 1. Experimental values of u_t/u_1 against u'_k/u_1 for $0.08 < KLe \leqslant 0.12$. ⊗, Abdel-Gayed *et al.* (1984); ◓, Abdel-Gayed *et al.* (1985); ○, Abdel-Gayed *et al.* (1988); ●, Andrews *et al.* (1975); -⊙-, Ballal (1979); ⊙, Ballal & Lefebvre (1975); ▽, Bollinger & Williams (1949); ⊠, Dandekar & Gouldin (1982); ▲, Grover *et al.* (1963); ◪, Hamamoto *et al.* (1984); k, Karlovitz (1954); K, Karlovitz *et al.* (1951); △, Karpov *et al.* (1959); ◒, Khramtsov (1959); ◥, Kido *et al.* (1983); ■, Petrov & Talantov (1959); ⊡, Singh (1975); ⊙, Smith & Gouldin (1978); ⧄, Sokolik *et al.* (1967); ∨, Vinckier & Van Tiggelen (1968); ◐, Wagner (1955); ∧, Williams *et al.* (1949); ⊗, Wohl & Shore (1955); Z, Zotin & Talantov (1966).

Figure 2. Experimental values of u_t/u_1 against u'_k/u_1 for $0.75 < KLe \leqslant 1.25$. (For key see figure 1.)

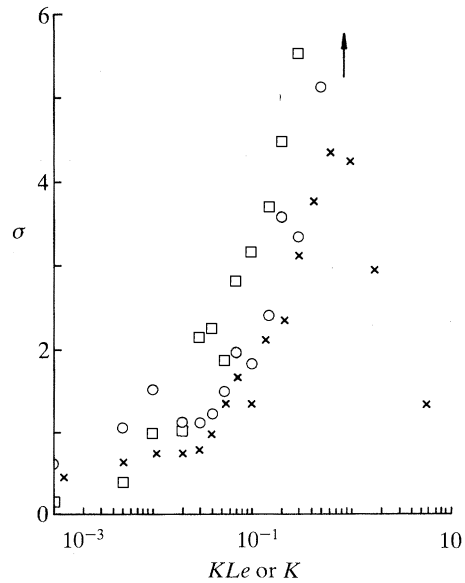

Figure 3. Mean deviations of experimental points from the correlation curve for different ranges of KLe and K. ×, KLe correlation; ○, K correlation ($Le \leqslant 1.3$); □, K correlation ($Le > 1.3$).

PHILOSOPHICAL TRANSACTIONS OF THE ROYAL SOCIETY A MATHEMATICAL, PHYSICAL & ENGINEERING SCIENCES

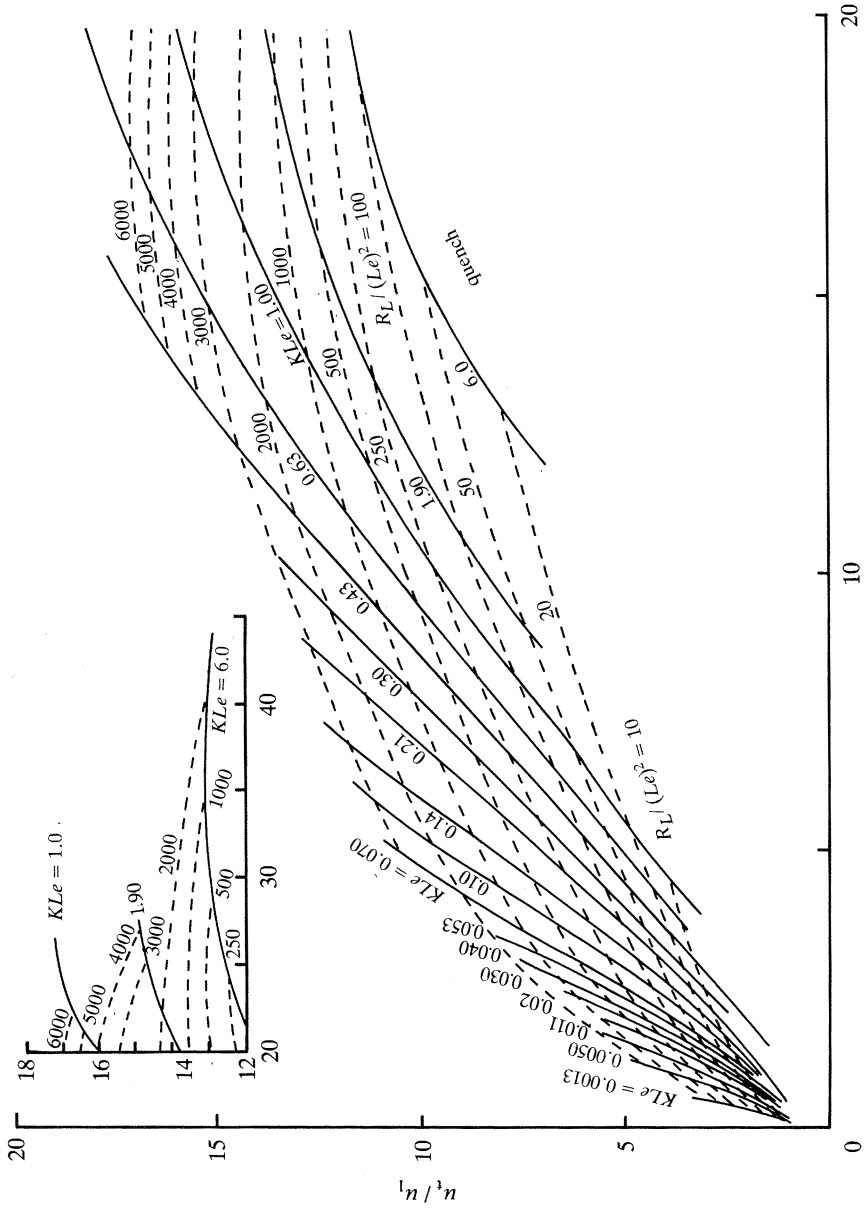

Figure 4. Smoothed data for u_t/u_1 against u_k'/u_1 at different stretch rates; dashed curves show $R_L/(Le)^2$.

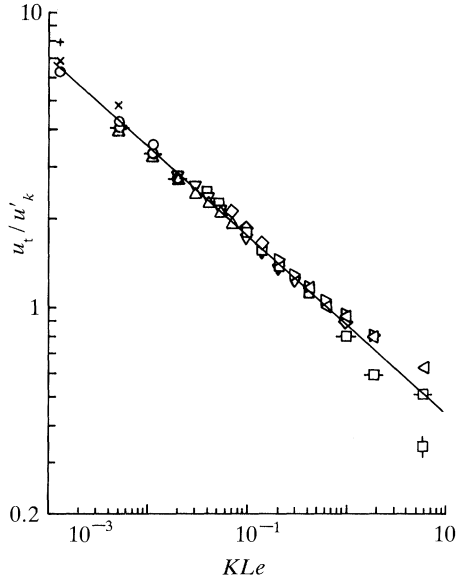

Figure 5. Experimental values of u_t/u'_k law at different values of KLe; solid line shows the power law $u_t/u'_k = 0.88\ (KLe)^{-0.3}$. u'_k/u_1: +, 0–0.2; ×, 0.2–0.4; ○, 0.4–0.6; ⊶, 0.6–1.0; △, 1.0–1.7; ▽, 1.7–2.5; □, 2.5–5.0; ◇, 5.0–7.0; ▷, 7.0–11; ◁, 11–18; ⊏, 18–30; ⊓, above 30.

graphical displays for different ranges of Le. Also shown on such graphs were curves for different values of R_L. In the light of the emergence of the KLe grouping, a correlation is presented in terms of this grouping, rather than in terms of K. The scatter of some experimental results when correlated in this way is shown by the plots of values of u_t/u_1 gainst u'_k/u_1 for two small ranges of KLe, first of 0.08 and 0.12 and then of 0.75 to 1.25 in figures 1 and 2, respectively. Further details about the experimental data are given in Abdel-Gayed & Bradley (1981) and Abdel-Gayed *et al.* (1984).

Whether the experimental points are indeed closer to the smoothed curves obtained by fitting a least squares curve through the experimental points for a given range of KLe or K values, to a correlation in terms of KLe, as we might expect, or to the original one in terms of K now is examined. Mean deviations, σ, of the experimental points from each curve, for different ranges of KLe and K were found from

$$\sigma = [\overline{(e-c)^2}]^{0.5}, \tag{13}$$

in which e is an experimental value and c is the corresponding value from the curve. The overbar indicates a mean value. These values, shown in figure 3, clearly indicate an improved correlation in terms of KLe.

Figure 4 presents the new correlation of all the available experimental data on a single graph in the form of smoothed curves at different values of KLe. Shown by the dashed curves are values of R_L/Le^2, which now becomes the appropriate expression of turbulent Reynolds number effects. These were obtained from a rearrangement of (2):

$$R_L/(Le)^2 = [0.157(u'/u_1)^2/KLe]^2. \tag{14}$$

As R_L is based upon u', such values correspond to $u'_k = u'$.

A further condensation of the data of figure 4 is given in figure 5 in the form of

logarithmic plots of u_t/u'_k against KLe. The influence of u'_k/u_l is relatively weak, particularly between $KLe = 0.01$ and 0.63. Within these limits, an approximate correlation is given by the equation of the straight line

$$u_t/u'_k = 0.88(KLe)^{-0.3}. \tag{15}$$

A very similar expression was used by Bray (1990) to correlate the data of Abdel-Gayed *et al.* (1987). As mentioned earlier, in the absence of flame stretch, the increase in flame area associated with flame wrinkling leads to an increase in u_t with u'_k. The observed decrease in u_t/u'_k with increase in KLe must be associated with the opposing influence of flame stretch.

4. Flame extinction stretch rates

(a) *Laminar flames*

In both experimental and theoretical studies of premixed laminar flames, the principal effect of stretch has been expressed through measured and computed values of the extinction, or quenching, stretch rate, s_q. This is the flame stretch, measured or computed, in the premixture at which a laminar flame is extinguished. The stretch depends upon the flow geometry and flame curvature. For example, (7) and (10) applied to flat flames in counter-flow, with cartesian coordinates and the X_1 direction normal to the flame surface, lead to the expression,

$$\frac{1}{A}\frac{\mathrm{d}A}{\mathrm{d}t} = \frac{\partial V_2}{\partial X_2} + \frac{\partial V_3}{\partial X_3}. \tag{16}$$

In this case there is no curvature and the flame stretch corresponds to that of a cold material surface parallel to the flame and moving into it. Because flame stretch rate cannot be measured directly, such expressions are necessary, to suggest the velocity gradient that should be either measured or computed to evaluate that rate. The continuity equation also can be invoked, in this case to show that the flame stretch rate in the cold premixture is given also by $-\partial V_1/\partial X_1$.

For flat flames arising from counter-flow from two, opposed, circular cross-section tubes, cylindrical coordinates are more appropriate with the flame surface in the diametral plane and the initial flow in the Z direction. This geometry is the one most frequently adopted in experimental and computational studies.

For such a circular cross-section flame, again with its surface on the X_2X_3-plane

$$X_1 = Z, \quad X_2 = R\sin\theta, \quad X_3 = R\cos\theta$$

and the transformation matrix is

$$L_{i\alpha} = \begin{pmatrix} L_{11} & L_{12} & L_{13} \\ L_{21} & L_{22} & L_{23} \\ L_{31} & L_{32} & L_{33} \end{pmatrix} = \begin{pmatrix} 1 & 0 & 0 \\ 0 & \sin\theta & \cos\theta \\ 0 & \cos\theta & -\sin\theta \end{pmatrix},$$

$$\boldsymbol{U} = (U_Z, U_R, U_\theta), \quad \mathrm{d}\boldsymbol{X} = (\mathrm{d}Z, \mathrm{d}R, R\mathrm{d}\theta).$$

All terms involving derivatives of the transformation matrix are zero, except

$$L_{j3}\,\partial L_{j2}/\partial X_3 = 1/R$$

and (7) leads to

$$\frac{1}{A}\frac{\mathrm{d}A}{\mathrm{d}t} = \frac{\partial V_R}{\partial R} + \frac{V_R}{R} + \frac{\partial V_\theta}{R\partial\theta}. \tag{17}$$

Again, the continuity equation may be invoked to show that in the cold premixture this is equal to $-\partial V_Z/\mathrm{d}Z$.

For radial flow into a circumferential flame, with the burnt gas moving in the axial direction

$$X_1 = R\cos\theta, \quad X_2 = R\sin\theta, \quad X_3 = Z$$

and the transformation matrix is

$$L_{i\alpha} = \begin{pmatrix} L_{11} & L_{12} & L_{13} \\ L_{21} & L_{22} & L_{23} \\ L_{31} & L_{32} & L_{33} \end{pmatrix} = \begin{pmatrix} \cos\theta & -\sin\theta & 0 \\ \sin\theta & \cos\theta & 0 \\ 0 & 0 & 1 \end{pmatrix},$$

$$\boldsymbol{U} = (U_R, U_\theta, U_Z), \quad \mathrm{d}\boldsymbol{X} = (\mathrm{d}R, R\mathrm{d}\theta, \mathrm{d}Z).$$

All terms involving derivatives of the transformation matrix are zero, except

$$L_{j2}\frac{\partial L_{j1}}{\partial X_2} = L_{12}\frac{\partial L_{11}}{\partial X_2} + L_{22}\frac{\partial L_{21}}{\partial X_2} + L_{32}\frac{\partial L_{31}}{\partial X_2} = \frac{1}{R}.$$

Therefore, (7) becomes

$$\frac{1}{A}\frac{\mathrm{d}A}{\mathrm{d}t} = \left(\frac{\partial U_\theta}{R\partial\theta} + \frac{\partial U_Z}{\partial Z}\right) + \frac{U_R}{R}. \tag{18}$$

For a stationary circumferential flame burning outwards $u_n = -V_R$ and $U_R = 0$. If $U_\theta = 0$, stretch arises entirely from the axial flow, with $U_Z = V_Z$.

For a spherical flame

$$X_1 = R\sin\theta\cos\phi, \quad X_2 = R\sin\theta\sin\phi, \quad X_3 = R\cos\theta,$$

$$L_{i\alpha} = \begin{pmatrix} L_{11} & L_{12} & L_{13} \\ L_{21} & L_{22} & L_{23} \\ L_{31} & L_{32} & L_{33} \end{pmatrix} = \begin{pmatrix} \sin\theta\cos\phi & \cos\theta\cos\phi & -\sin\phi \\ \sin\theta\sin\phi & \cos\theta\sin\phi & \cos\phi \\ \cos\theta & -\sin\theta & 0 \end{pmatrix},$$

$$\boldsymbol{U} = (U_R, U_\theta, U_\phi), \quad \mathrm{d}\boldsymbol{X} = (\mathrm{d}R, R\mathrm{d}\theta, R\sin\theta\,\mathrm{d}\phi).$$

All terms involving derivatives of the transformation matrix are zero, except

$$L_{j3}\,\partial L_{j2}/\partial X_3 = \cot\theta/R, \quad L_{j2}\,\partial L_{j1}/\partial X_2 = L_{j3}\,\partial L_{j1}/\partial X_3 = 1/R$$

and (7) becomes

$$\frac{1}{A}\frac{\mathrm{d}A}{\mathrm{d}t} = \left(\frac{\partial U_\theta}{R\partial\theta} + \frac{\cot\theta}{R}U_\theta + \frac{\partial U_\phi}{R\sin\theta\partial\phi}\right) + \frac{2U_R}{R}. \tag{19}$$

Usually $U_\theta = U_\phi = 0$. For a stationary flame burning outwards $u_n = -V_r, U_r = 0$ and there is no stretch. For an outwardly propagating explosion flame, the stretch is twice the flame speed $(u_n + V_r)$ divided by the flame radius.

Because counter-flowing flat flames have most frequently been used to measure or compute values of s_q, concentration is centred on these. The values obtained depend on whether two cold streams are counter-flowing into the flame (symmetric flow) or whether one stream consists of burnt products at the adiabatic temperature (asymmetric flow).

In the latter case the definition of s_q is not as clear cut. There is, for example, no sharp cut off in volumetric heat release rate with increasing stretch, only a gradual

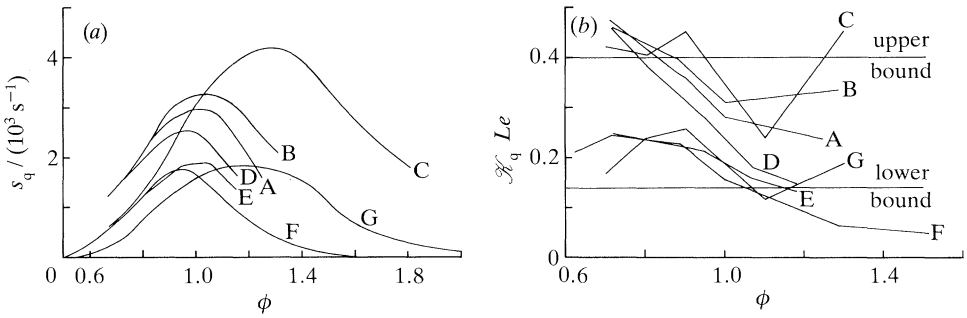

Figure 6. Variation of quenching stretch rate for laminar flames with mixture and equivalence ratio, (*a*) in terms of s_q, (*b*) in dimensionless form. See text for key.

decrease (Bradley & Lau 1990). Law *et al.* (1988) measured s_q for various laminar methane–air and propane–air premixed flames in symmetric counter-flow from two identical high contraction nozzles of circular cross section. The velocity gradient in the gases approaching the flame yielded the stretch rate as given by (17), and a value of s_q at extinction. On the basis of chemical kinetic models of flat, essentially one-dimensional laminar flames, Dixon-Lewis (1988*b*), Stahl *et al.* (1988), and Kee *et al.* (1988) and Stahl & Warnatz (1991) have computed theoretical values of s_q, again in counter-flow. Stahl *et al.* obtained values for CH_4–air and C_3H_8–air mixtures and considered flat flames with symmetric counter-flows, in one case for an infinite planar slab and in another case for a circular cross section. The latter was used in the experiments of Law *et al.* Kee *et al.* modelled circular cross section symmetric counterflows with CH_4–air mixtures and used two methods, the traditional analysis in which the stretch field is characterized by a single parameter, the potential-flow velocity gradient, and an alternative formulation which represents the flow field more accurately. The alternative formulation is the more appropriate for modelling the experiments of Law *et al.* (1988). Stahl & Warnatz (1991) have extended their earlier work for CH_4–air mixtures to include *C*3 chemistry.

Figure 6*a* shows, for the circular cross section symmetric counter-flow configuration, the variations of s_q with equivalence ratio, ϕ, for CH_4 and C_3H_8–air mixtures obtained by these workers. The computed values of Stahl & Warnatz (1991) for CH_4–air mixtures are shown by curve A, those of Stahl *et al.* (1988) for the circular cross section, with CH_4–air and C_3H_8–air mixtures by curves B and C respectively, those for CH_4–air mixtures for the traditional and alternative formulations of Kee *et al.* (1988) by curves D and E and those for the experiments with CH_4–air and C_3H_8–air mixtures of Law *et al.* (1988) by curves F and G. In general, the theoretical values of s_q are higher than those measured. No experimental or theoretical data on s_q for the asymmetric counter-flow configuration are available.

In line with the discussion in the previous section, greater generality is sought for the values of flame extinction stretch rates through the product of a dimensionless stretch rate and Lewis number. Following the procedure adopted for turbulent flames, the laminar flame stretch rate is normalized by u_l/δ_l to define a dimensionless group, $\mathscr{K}_q$, to express the laminar flame extinction stretch rate, such that

$$\mathscr{K}_q = s_q \delta_l / u_l. \tag{20}$$

Values of u_l for CH_4–air mixtures were taken from Andrews & Bradley (1972).

Those for C_3H_8–air were obtained from those presented by Abdel-Gayed *et al.* (1985) for a temperature of 328 K, corrected by the expression of Metghalchi & Keck (1982) for a temperature of 298 K. Values of Le were obtained from Abdel-Gayed *et al.* (1985) and of δ_l were given by $\delta_l = \nu/u_l$. Shown in figure 6*b* are values of $\mathscr{K}_q Le$ found in this way. Although not perfect, some generality in the quenching data is exhibited when the grouping $\mathscr{K}_q Le$ is used. The rather randomized scatter is probably associated with uncertainties in the value of Le. The horizontal lines in figure 6*b* represent upper and lower bounds of 0.40 and 0.14 and they indicate approximate limits of uncertainty. A generalized value of $\mathscr{K}_q Le$, at least for paraffinic fuels with air, might be expected to lie within these limits.

(*b*) *Turbulent flames: distribution of flamelet stretch rates*

Several problems arise in the utilization of laminar flame extinction stretch rate data in the flamelet modelling of turbulent combustion. One concerns the most appropriate laminar flow configuration to represent turbulent combustion conditions. Because in the régime of partial turbulent flame quenching some burnt gas is always present, potentially to sustain the flame, it would seem more appropriate to use quenching stretch rate databased upon the laminar asymmetric, rather than the symmetric, counter-flow condition. Another problem concerns the magnitude of the relevant stretch rate with turbulent combustion. Even with isotropic turbulence the eulerian mean strain rate, u'/λ, is not a direct measure of the lagrangian flow field stretch rate to which the flame is subjected. In addition, the distribution of stretch rates about the mean must be known.

Because, in turbulent flow, both material line and surface elements on average tend to increase and because material lines appear to flow in the direction in which strains are positive, two of us (Abdel-Gayed *et al.* 1989*a*) postulated that line elements at the flame surface tended towards the axis of maximum principal strain rate. This enabled the flame stretch rate to be expressed in terms of the maximum strain rate. From experimentally measured PDFs of eulerian strain rates in isothermal flow, it was then possible to derive lagrangian PDFs of the flame surface strain rate.

Such PDFs when taken in conjunction with schlieren photographs of turbulent flames that were quenching in a fan-stirred explosion vessel, implied flame extinction stretch rates that were significantly higher than those either measured or computed for laminar flames with symmetric counter-flow. One explanation of this is that the strain rate was overestimated by the assumption that the line elements align with the axis of maximum strain rate and in the discussion of this work Pope (1989) reported a 30% probability of negative strain rates on material surface elements, on the evidence of direct computerized numerical simulations of turbulence.

Subsequently, Yeung *et al.* (1990) published further results of their simulations for constant density, homogeneous, isotropic turbulence. In figs 6 and 7 of their paper they give PDFs of stretch rates, s, normalized by the Kolmogorov time, τ_η, for a Reynolds number, R_λ, of 93, based on the Taylor microscale. Over a range of values of R_λ from 38 to 93 there was virtually no Reynolds number dependence. Two of these PDFs, from their figure 7 for $R_\lambda = 93$, are reproduced in figure 7. The PDF of the total stretch rate, a, in the tangent plane of a material surface is indicated by $f(a)$, while that, α, for a randomly orientated surface element (not a material one) is indicated by $f(\alpha)$. The stretch rates a and α are dimensionless and given by $s\tau_\eta$.

The former PDF exhibits a 20% probability of a negative rate of stretch, while the latter is symmetrical about zero and has a variance, σ_α^2, that is close to the theoretical

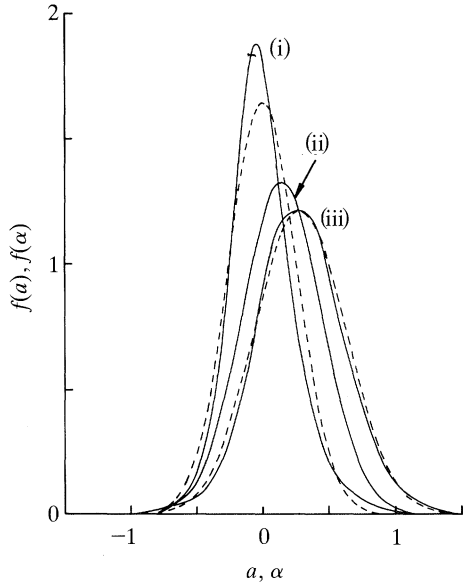

Figure 7. Stretch rate PDFs for material, randomly orientated and intermediate surfaces. Broken curves are gaussian curve fits. (i) $f(\alpha)$ random surface, zero mean, r.m.s. = 0.257. (ii) Intermediate surface, $KLe = 0.02$. (iii) $f(a)$ material surface, mean = 0.283, r.m.s. = 0.341.

value of $\frac{1}{15}$ for an eulerian distribution of stretch rates. This value follows from a consideration of the mean value of the specific dissipation rate of the turbulent energy, ϵ. For homogeneous, isotropic turbulence this is related to u'/λ by (Taylor 1935)

$$\epsilon/\nu = 2\overline{s_{ij}\, s_{ij}} = 15\overline{(\partial u/\partial x)^2} = 15(u'/\lambda)^2, \tag{21}$$

in which s_{ij} is the strain rate tensor. Because $\tau_\eta = (\nu/\epsilon)^{0.5}$ it follows that the variance $(u'/\lambda)^2 \tau_\eta^2 = \frac{1}{15}$.

The broken curves on figure 7 are gaussian distributions for the same values of mean and variance as in the PDFs of Yeung *et al.* (1990). The derived and gaussian PDFs are not identical, and Yeung *et al.* discuss the differences in detail. However, these are not great and with sufficient accuracy, as well as convenience, in the present work a gaussian PDF is assumed. In dimensional form, this is

$$p(s) = \frac{1}{(2\pi)^{\frac{1}{2}}\sigma_s} \exp\left[-\left(\frac{s-\bar{s}}{2^{\frac{1}{2}}\sigma_s}\right)^2\right] \tag{22}$$

with σ_s the r.m.s. rate of stretch and $\bar{s}$ the mean value. Over the range of values of R_λ between 38 and 93, the average values of $\bar{s}\tau_\eta$ and $\sigma_s \tau_\eta$, in the simulations of Yeung *et al.* (1990), are 0.280 and 0.341 for a material surface, and 0 and 0.257 for a randomly orientated one. From $\tau_\eta = (\nu/\epsilon)^{0.5}$ and substitution in terms of u'/λ from (21)

$$\bar{s} = 1.08u'/\lambda = 0.279(\epsilon/\nu)^{0.5}, \tag{23}$$

$$\sigma_s = 1.32u'/\lambda = 0.341(\epsilon/\nu)^{0.5}, \tag{24}$$

for a material surface, and

$$\bar{s} = 0, \tag{25}$$

$$\sigma_s = u'/\lambda = (\tfrac{1}{15}\epsilon/\nu)^{0.5}, \tag{26}$$

for a randomly orientated one. As discussed above, this latter pair of values is to be expected for an eulerian distribution of stretch rates.

A laminar flamelet is a propagating surface element and as the flame propagation velocity becomes small relative to turbulent velocities, at large values of KLe, the flame surface element will tend towards that of a material surface. On the other hand, as the flame propagation velocity becomes relatively higher, at small values of KLe, the flame surface element becomes more randomly orientated. Yeung *et al.* suggested that the stretch rate on a flame surface might be assumed to be similar to that on a material surface when the laminar burning velocity becomes greater than the Kolmogorov velocity. Expressed in the present terminology, this is equivalent to $K \geqslant 0.258$. For both types of surface the distribution is very close to the gaussian distribution given by (22).

To express the transition between a randomly orientated flame surface at $KLe = 0$ and a material surface when KLe is greater than 0.258 an empirical exponential form is proposed given by

$$\bar{s} = [1.08 \exp -(a/KLe)]\, u'/\lambda, \tag{27}$$

$$\sigma_s = [1 + 0.32 \exp -(a/KLe)]\, u'/\lambda, \tag{28}$$

in which a is a stretch dependency factor, here assigned the value of 0.0132. With this value, when $KLe = 0$ the randomly orientated surface relationships, (25) and (26) are recovered, whereas when $KLe = 0.258$, $\bar{s}$ is 95% and σ_s is 99% of the respective values for a material surface given by (23) and (24). Also shown in figure 7 is a gaussian PDF when $KLe = 0.02$, and when $\bar{s}$ and σ are given by (27) and (28) with $a = 0.0132$.

(*c*) *Turbulent flames: extinction stretch rates from heat release rate profiles*

Here the concept of a turbulent flame extinction stretch rate is introduced via the effect of flame stretching on the volumetric heat release rate–temperature profile. Such profiles for the laminar flames of particular premixtures are used as inputs in some mathematical models of combustion (Bradley *et al.* 1987, 1988*a*, 1991; Bradley & Lau 1990; Abd Al-Masseeh *et al.* 1991*a*, *b*). The treatment that follows relates to such modelling, as well as to the present interpretation of turbulent burning velocities. The extinction stretch rate is featured as an important parameter, not only in this, but also in other types of flamelet models such as, for example, those associated with Bray and co-workers, even though these adopt a somewhat different treatment of chemical reaction. The model of Bray *et al.* (1985), assumes the flame sheet to be thin and the gas to be either burnt or unburnt ($K = 0$). More recently, Bray and co-workers have expressed the reaction rate in terms of flamelet surface to volume ratio and flamelet crossing frequency at a fixed point (Bray *et al.* 1988, 1989), with an allowance for the effects of flame stretch (Cant *et al.* 1991).

The approach based on the heat release profile utilizes a reaction progress variable, or reactedness, θ, defined by the dimensionless temperature rise, $(T - T_u)/(T_b - T_u)$, in which T is the gas temperature and the subscripts u and b indicate unburnt and burnt gas conditions. Values range from 0 on the unburnt side to 1 on the burnt side. For each particular temperature and initial mean stretch rate, there is a

PHILOSOPHICAL TRANSACTIONS OF THE ROYAL SOCIETY A MATHEMATICAL, PHYSICAL & ENGINEERING SCIENCES

corresponding, single valued, volumetric heat release rate, $q_l(\theta, s)$, which, in accordance with the flamelet assumption, is taken to be the same as that in a laminar flame of the same premixture and stretch rate. A joint PDF, $p(\theta, s)$, is associated with the fluctuations in both θ and s.

The mean, mass weighted, volumetric heat release rate at a given point in the turbulent flame is

$$\tilde{q}_t = \int_{-\infty}^{\infty} \int_0^1 q_l(\theta, s)\, p(\theta, s)\, \mathrm{d}\theta\, \mathrm{d}s. \tag{29}$$

There is currently no means of accurately evaluating $p(\theta, s)$ and the computationally attractive approximation is made that stretch rates are uncorrelated with θ and the joint PDF is the product of the separated PDFs, $p(\theta)$ and $p(s)$. Equation (29) becomes

$$\tilde{q}_t = \int_{-\infty}^{\infty} \int_0^1 q_l(\theta, s)\, p(\theta)\, p(s)\, \mathrm{d}\theta\, \mathrm{d}s. \tag{30}$$

In the case of symmetric counter-flowing laminar flames, discussed earlier, an extinction stretch rate is sharply defined. Bradley & Lau (1990) show laminar heat release rate versus θ profiles, computed by Dixon-Lewis & Missaghi from mathematical models with detailed chemical kinetics (Dixon-Lewis & Islam 1982; Dixon-Lewis 1988*a*, *b*), that hardly change with s until an extinction stretch rate, s_q, is attained, above which value there is no heat release. At present, little is known about the influence of any component of negative stretch rate. This is an area which requires experimental and computational study. For the present it is assumed that for all such values the associated heat release rate is the same as at zero stretch. With this condition and the assumption that the heat release rate profile is unchanged by stretch until s_q is attained, beyond which value there is no heat release, (30) can be rewritten in the more tractable form:

$$\tilde{q}_t = \int_{-\infty}^{s_q} p(s)\, \mathrm{d}s \int_0^1 q_l(\theta)\, p(\theta)\, \mathrm{d}\theta. \tag{31}$$

For the case of the asymmetric laminar flame counter-flowing against adiabatic combustion products, also discussed earlier, Bradley & Lau (1990) show heat release rate profiles, again obtained by Dixon-Lewis & Missaghi, which change in a more gradual way with increasing initial stretch rate. Because (31), and the concept of a 'top hat' heat release profile with a well-defined extinction stretch rate, are more convenient to use than is (30) in computations, and because the asymmetric counter-flow is probably more realistic for turbulence modelling than is the symmetric counter-flow condition, it is convenient to introduce a turbulent extinction stretch rate, s_{qt}, defined by an equalization of (30) and (31):

$$\int_{-\infty}^{s_{qt}} p(s)\, \mathrm{d}s \int_0^1 q_l(\theta)\, p(\theta)\, \mathrm{d}\theta = \int_{-\infty}^{\infty} \int_0^1 q_l(\theta, s)\, p(\theta)\, p(s)\, \mathrm{d}\theta\, \mathrm{d}s = \tilde{q}_t. \tag{32}$$

The complex equation (32) requires numerical solution to obtain s_{qt} and values of this parameter were obtained only for those heat release profiles at different stretch rates of Dixon-Lewis & Missaghi, to which reference already has been made, but for both types of counterflow. The mixture comprised methane–air of equivalence ratio 0.84 at one atmosphere pressure (*ca.* 10^5 Pa) and a temperature of 288 K. The computations covered a range of premixture mean stretch rates with the distribution

Figure 8

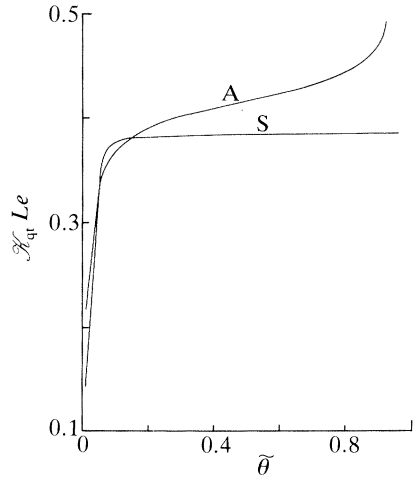

Figure 9

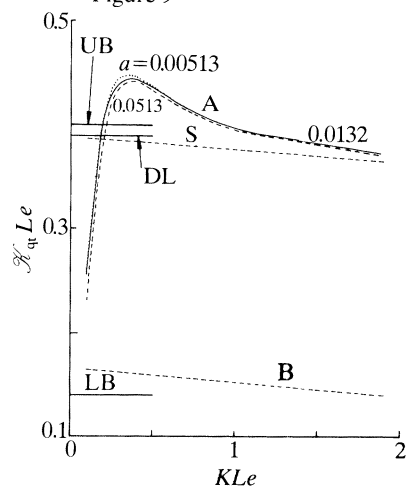

Figure 8. Values of $\mathscr{K}_{qt}Le$ at different values of $\tilde{\theta}$ for symmetric (S) and asymmetric (A) counter-flow configurations. $KLe = 0.24$.

Figure 9. Values of $\mathscr{K}_{qt}Le$ at different values of KLe for symmetric (S) and asymmetric (A) counter-flow configurations with different PDFs of stretch rate. $\tilde{\theta} = 0.6$. UB, Upper bound; LB, lower bound; DL, s_q (Dixon-Lewis 1988*b*).

of (22) over a range of Favre, or mass weighted, mean values of the reaction progress variable, $\tilde{\theta}$. Values of $\bar{s}$ and σ_s were obtained from (27) and (28) with $a = 0.0132$.

In the mathematical modelling of turbulent combustion $p(\theta)$ is usually represented by a beta function defined by its first ($\tilde{\theta}$) and second ($\tilde{\theta}''^2$) moments. Unfortunately, there is currently little experimental validation of this assumption, although much effort is being expended on it. Problems include the finite measuring volume in laser diagnostics (Lawes 1991) and the difficulties of compensating for thermal inertia in thermocouple thermometry (Bradley *et al.* 1989*b*). For infinitely fast reaction ($u_l = \infty, K = 0$) Lewis & Moss (1979) have derived a simple relationship between $(\tilde{\theta}''^2)^{0.5}$ and θ. Abdalla *et al.* (1982) have presented experimental curves of $(\theta''^2)^{0.5}$ plotted against $\tilde{\theta}$, under an envelope of the curve of Lewis & Moss, for different values of a parameter that reduces to $6.37Ku_l/u'$. Despite the measurement limitations, these relationships were used, after some smoothing and extrapolation to higher values of K, to evaluate $(\tilde{\theta}''^2)^{0.5}$ for given values of KLe and $\tilde{\theta}$. The beta function assumed for $p(\theta)$ was evaluated from the two moments.

Values of s_{qt} were obtained from (32) and, following the procedures adopted for s_q to obtain greater generalization, were normalized and multiplied by the value of Le to give $\mathscr{K}_{qt}Le$. Shown in figure 8 are the values of $\mathscr{K}_{qt}Le$, computed in this way for the symmetric and asymmetric circular cross section counter-flow configuration when $KLe = 0.24$ plotted against $\tilde{\theta}$, for this mixture.

The concept of a single-valued turbulent flame extinction stretch rate, s_{qt}, or in dimensionless terms $\mathscr{K}_{qt}Le$, is better fulfilled by the results from the symmetric counter-flow condition than by those from the asymmetric, burnt gas, counter-flow condition. This is not surprising, because in the former case the laminar flame heat release rate–temperature profile is almost unchanged as the stretch rate is increased up to the extinction rate, when the heat release falls to zero: whereas in the latter

case the shape of the profile changes significantly as the stretch rate is increased and no sharply defined extinction point is observed (Bradley & Lau 1990). However, even for the symmetric case, there is some dependence of $\mathscr{K}_{qt}Le$ upon both $\tilde{\theta}$ and KLe.

Because it is computationally attractive to use the parameter s_{qt} for s_q in (31) it is necessary not only to recognize that $\mathscr{K}_{qt}Le$ must be a function of KLe, but also to ascribe a value of $\tilde{\theta}$ at which the value of $\mathscr{K}_{qt}Le$ be designated. In view of the importance of the reaction zone, associated with the higher values of $\tilde{\theta}$, the value of 0.6 was arbitrarily selected for both flow conditions. Shown in figure 9 are computed values of $\mathscr{K}_{qt}Le$ at this value, for different values of KLe and both types of counter-flow.

To demonstrate the effect of a change in the transition of the stretch rate PDF, (22), from the randomly orientated to the material surface condition the value of the numerical constant a in (27) and (28) was changed from 0.0132 to 0.00513 and 0.0513. The second and third values gave corresponding values of $\bar{s}$ that were 95% that of the material surface value given by (23) with $KLe = 0.1$ and $KLe = 1.0$ respectively. The corresponding computed values of $\mathscr{K}_{qt}Le$ are shown by the dotted curve for $a = 0.00513$ and by the dashed curve for $a = 0.0513$ in figure 9. These curves are for the asymmetric, burnt gas, counter-flow condition, the one that seems to be more appropriate for turbulent flames. The computed values of $\mathscr{K}_{qt}Le$ in figure 9 are used in the investigations of the effects of flame quenching upon turbulent burning velocity in the next section.

Also indicated are the extinction stretch rates for laminar flames for this mixture computed by Dixon-Lewis & Missaghi and the upper and lower bounds values of 0.40 and 0.14, previously shown in figure 6*b*.

5. Turbulent burning velocities in terms of flame extinction stretch rates

In turbulent combustion, where a discernable flame front exists, it is defined by the mean surface that separates cold premixture and hot gases. Because of flame stretch, in the partially quenched régime of flame propagation, at any instant only a proportion of the mean flame front area will be propagating. Following Abdel-Gayed *et al.* (1989*a*), let this ratio be A_r. This implies that of the unburnt gas contiguous with the flame front, this proportion must be experiencing a stretching rate on the appropriate surface element that is less than s_{qt}. This effect is diagrammatically illustrated by the stretch rate distribution in figure 10 with a given value of s_{qt}. The shaded area represents A_r.

$$A_r = \int_{-\infty}^{s_{qt}} p(s)\,\mathrm{d}s. \tag{33}$$

With $p(s)$ given by (22)

$$A_r = \tfrac{1}{2}[1 + \mathrm{erf}\,((s_{qt} - \bar{s})/2^{\frac{1}{2}}\sigma_s)], \quad \text{for} \quad s_{qt} > \bar{s}, \tag{34}$$

$$= \tfrac{1}{2}[1 - \mathrm{erf}\,((\bar{s} - s_{qt})/2^{\frac{1}{2}}\sigma_s)], \quad \text{for} \quad s_{qt} \leqslant \bar{s}, \tag{35}$$

where the error function is given by

$$\mathrm{erf}\,(y) = \frac{2}{\sqrt{\pi}} \int_0^y \mathrm{e}^{-x^2}\,\mathrm{d}x \tag{36}$$

and $\bar{s}$ and σ_s are given by (27) and (28).

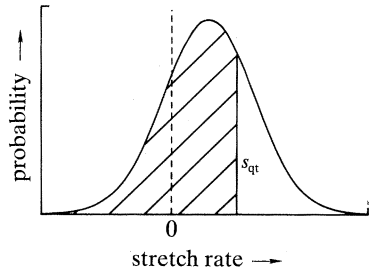

Figure 10. Stretch rate PDF, showing proportion of spectrum that supports combustion.

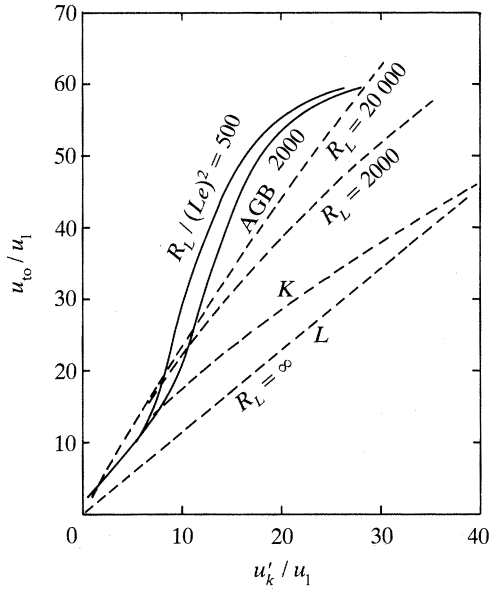

Figure 11. Values of u_{to}/u_1 against u'_k/u_1 at different values of R_L or $R_L/(Le)^2$. Solid curves are present predictions, broken lines previous theories. AGB, Abdel-Gayed & Bradley (1981); K, Klimov (1983); L, Libby *et al.* (1979).

In pursuit of maximum generality through the use of dimensionless groups it is convenient to normalize stretch rates, s, by u_1/δ_1 to give

$$\mathscr{K} = s\delta_1/u_1. \tag{37}$$

Furthermore, the dimensionless group $\mathscr{K} Le$ is more general than is $\mathscr{K}$ alone. When stretch rates are normalized by u_1/δ_1 and multiplied by Le, (34) and (35) give

$$A_r = \frac{1}{2}\left[1+\operatorname{erf}\left(\frac{\mathscr{K}_{qt}Le-\bar{\mathscr{K}}Le}{2^{\frac{1}{2}}\sigma_{\mathscr{K}}Le}\right)\right], \quad \text{for} \quad \mathscr{K}_{qt}Le > \bar{\mathscr{K}}Le, \tag{38}$$

$$= \frac{1}{2}\left[1-\operatorname{erf}\left(\frac{\bar{\mathscr{K}}Le-\mathscr{K}_{qt}Le}{2^{\frac{1}{2}}\sigma_{\mathscr{K}}Le}\right)\right], \quad \text{for} \quad \mathscr{K}_{qt}Le \leqslant \bar{\mathscr{K}}Le, \tag{39}$$

and (27) and (28) give

$$\bar{\mathscr{K}}\,Le = [1.08\exp-(a/KLe)]\,KLe, \tag{40}$$

$$\sigma_{\mathscr{K}}\,Le = [1+0.32\exp-(a/KLe)]\,KLe. \tag{41}$$

With the binary approach, implicit in the use of $\mathscr{K}_{qt}$ for a given mixture, that combustion either does or does not occur depending upon the localized value of the stretch rate, the ratio u_t/u_l must be proportional to the fraction of the total flame front area that is supporting flame propagation. It is demonstrated by figure 9 that for a given flow condition and value of a in (40) and (41), $\mathscr{K}_{qt}\,Le$ is a function solely of KLe. Thus KLe determines the value of the ratio A_r, given by (38) and (39). If there were no extinction, $s_{qt}=\infty$ and $\mathscr{K}_{qt}=\infty$, or more generally $\mathscr{K}_{qt}\gg\mathscr{K}$, then A_r would be the area under the full PDF curve in figure 10, namely unity. If u_{to} be an imaginary turbulent burning velocity that would obtain were there no extinction due to flame stretch, it follows that

$$(u_t/u_l)/(u_{to}/u_l)=A_r. \tag{42}$$

A value of KLe was selected, corresponding to one of the values on the correlation graph of figure 4, and the value of A_r found from (38) to (41). Along the curve of constant KLe, at different values of u'_k/u_l the corresponding values of u_{to}/u_l were found from the associated values of u_t/u_l and (42).

Shown by the full line curves in figure 11 are values of u_{to}/u_l plotted against u'_k/u_l that were generated in this way for the asymmetric, burnt gas, counter-flow condition with the presently computed values of $\mathscr{K}_{qt}\,Le$ in figure 9 and a value of the stretch dependency factor, a, equal to 0.0132. Such curves, only two of which are drawn here, for $R_L/Le^2=500$ and 2000, show but slight dependence upon either this grouping or KLe. Indeed, no such dependency is to be expected, because stretch rate effects are absent at zero stretch rate, a condition attained when R_L is infinite. Furthermore, as discussed in §1, flame wrinkling in the absence of stretch leads to a near-linear relationship between u_t and u'_k with no influence of the length scale.

Also shown in figure 11 are values predicted by earlier stretch-free theories of turbulent burning. The predictions of Abdel-Gayed & Bradley (1981) and Libby *et al.* (1979) are slightly influenced by R_L. Broken curves for values of R_L of 20000 and 2000 are shown for the predictions of Abdel-Gayed & Bradley, for a value of $R_L=\infty$ for the predictions of Libby *et al.*, while those of Klimov (1983) are independent of R_L. All of these predictions of u_{to}/u_l are lower than the present values. This is because none of the theories is self-contained and all require recourse to experimental values of turbulent burning velocities which are, in fact, affected by flame stretch. Abdel-Gayed & Bradley did this to determine a turbulence intermittency factor, while Libby *et al.* evaluated a constant to account for uncertain features in both the thermochemical and fluid mechanical modelling. Klimov determined the value of a constant to account for non-uniformities in the width of interstices between flame fronts.

The closeness of overlapping portions of generating curves of u_{to}/u_l for different values of KLe to a best fit curve of u_{to}/u_l against u'_k/u_l is testimony to the consistency of the interpretation of the measured values of u_t/u_l in figure 4 in terms of the PDF of stretch rates and s_{qt}. Such curves are shown by the dashed lines in figure 12 for the same conditions as figure 11. Another convenient way of presenting the same data is shown in figure 13. Here separate points present values of A_r that have been derived from the experimental data of figure 4 and the best curve of u_{to}/u_l

PHILOSOPHICAL TRANSACTIONS OF THE ROYAL SOCIETY A MATHEMATICAL, PHYSICAL & ENGINEERING SCIENCES

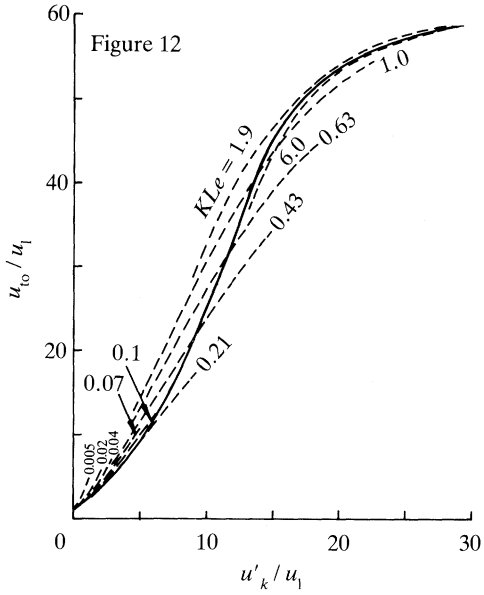

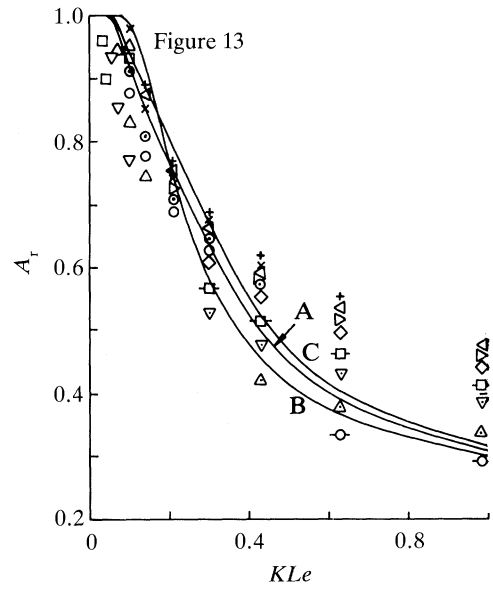

Figure 12. Values of u_{to}/u_1 against u'_k/u_1. Broken curves represent different values of KLe and the solid curve, a best fit.

Figure 13. Values of A_r against KLe. Symbols represent different values of u'_k/u_1 for the asymmetric counter-flow configuration and $a = 0.0132$. (□, 1.0; ▽, 1.5; △, 2.0; ○, 2.5; ⊙, 3; ×, 4; +, 5; ◁, 6; ▷, 7; ◇, 8; ⊟, 9; ▽, 10; △, 11; ⊸, 12.) Solid curves are predicted values. Curve A, asymmetric, $a = 0.0132$; curve B, symmetric, $a = 0.0132$; curve C, asymmetric, $a = 0.0513$.

shown in figure 12 using (42). The full line curve labelled A shows completely theoretical values of A_r given solely by (38)–(41), again with the computed asymmetric values of $\mathscr{K}_{qt}Le$ and a value of a of 0.0132. The closeness of this to the experimental points is satisfactory. To check the sensitivity of the assumed counter-flow configuration the theoretical curve B was constructed for the computed values of $\mathscr{K}_{qt}Le$ for symmetric counter-flow. Its closeness to curve A suggests solutions are not so sensitive to this assumption, but agreement with experiment is somewhat better at low values of KLe with the asymmetric assumption.

As discussed in §4*b*, a value of a of 0.0132 expresses a transition from a stretch rate PDF appropriate to a randomly orientated flame surface element at $KLe = 0$ to one appropriate to a material surface at $KLe = 0.258$. There is no direct numerical or experimental evidence on this transition for a flame, but the present data might provide some guidance. To this end, values of a equal to 0.00513 and 0.0513 were substituted in (38)–(41). The former gave values of A_r very close to those obtained with $a = 0.0132$ over the full range of KLe. A value of 0.0513 gave, for the axisymmetric counter-flow condition, the full line curve C in figure 13. This value of a gives a value of $\bar{s}$ in (27) which is 95% of the value for a material surface when $KLe = 1$. The agreement with the experimental points is not as good as with the smaller values of a.

Another uncertainty is the most appropriate value of $\mathscr{K}_{qt}Le$ at the different values of KLe, bearing in mind the range of laminar flame extinction stretch rates, evidenced in figure 6, that have been computed or measured by different workers. The presently computed values of $\mathscr{K}_{qt}Le$ are based upon a value of s_q close to the

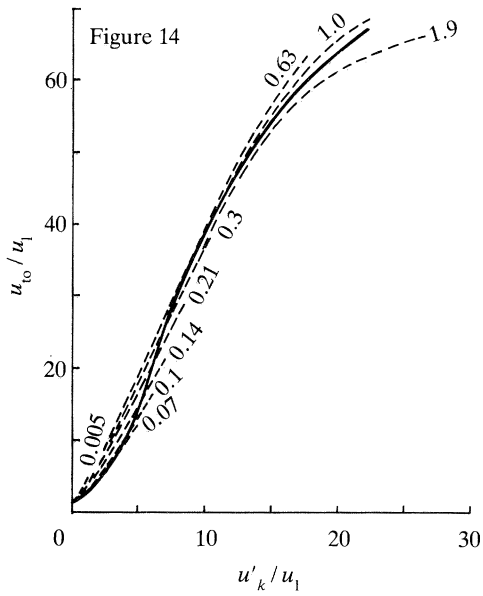

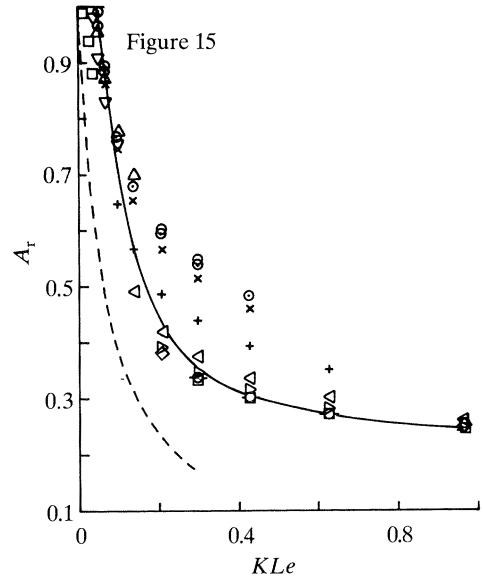

Figure 14. Values of u_{to}/u_1 against u'_k/u_1. Broken curves represent different values of KLe and the solid curve, a best fit. Asymmetric, $a = 0.0132$. $\mathscr{K}_{qt}Le = 0.166 - 0.014KLe$.

Figure 15. Values of A_r against KLe. The symbols represent different values of u'_k/u_1 for the asymmetric counter-flow configuration and $a = 0.0132$. The solid line represents predicted values. Asymmetric, $a = 0.0132$, $\mathscr{K}Le = 0.166 - 0.014KLe$. See figure 13 for key. ----, Bray (1990), $\sigma = 2.0$.

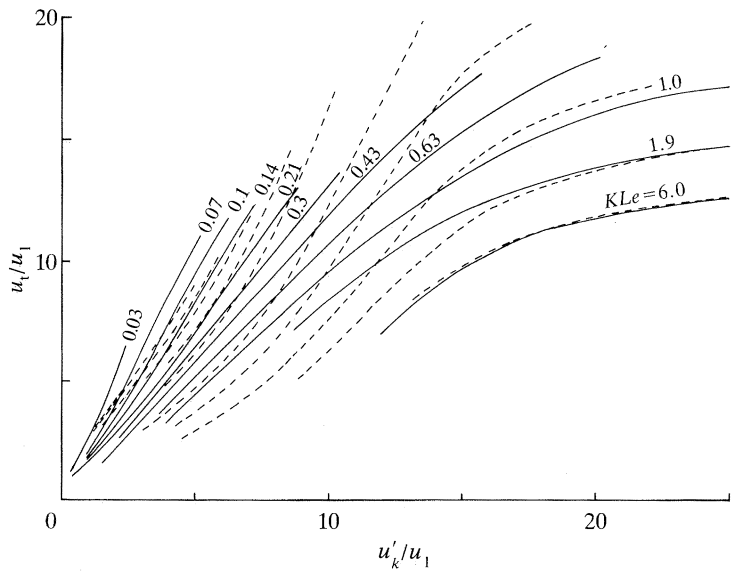

Figure 16. Smoothed data for u_t/u_1 against u'_k/u_1 at different stretch rates; solid curves are experimental; broken curves are predicted from u_{to}/u_1 in figure 12, full line curve in figure 9.

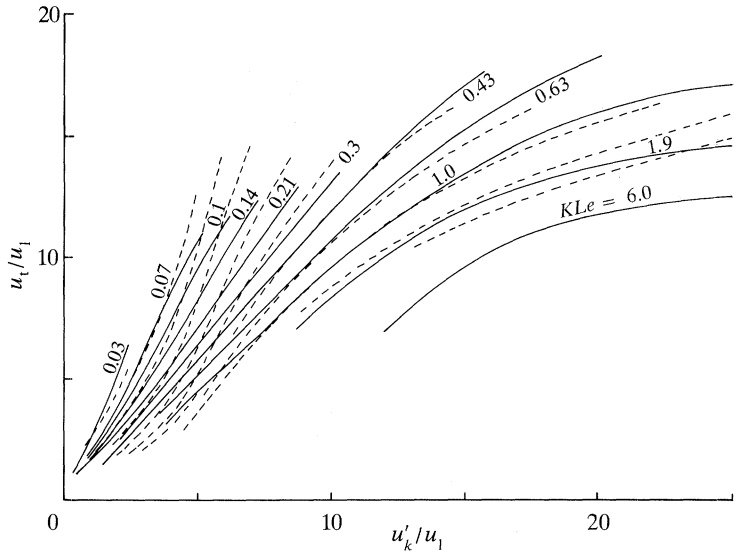

Figure 17. Smoothed data for u_t/u_l against u'_k/u_l at different stretch rates; solid curves are experimental; broken curves are predicted from u_{to}/u_l in figure 14 and (43).

upper bound on the figure. To explore the possibility of better agreement between experimental points and theoretical prediction, the computed asymmetric condition curve of $\mathscr{K}_{qt}Le$ on figure 9 was substituted by one shown by the broken line B. This is close to the mean experimental value of 0.16 given by the results of Law *et al.* (1988). Its equation is

$$\mathscr{K}_{qt}Le = 0.166 - 0.014KLe. \tag{43}$$

Again with $a = 0.0132$ this gave rise to the curves of u_{to}/u_l against u'_k/u_l on figure 14 and the plot of A_r against KLe on figure 15. It is clear from the latter and a comparison of figure 14 with figure 12 that this condition gives better agreement with the measured turbulent burning velocities than does the originally computed curve for asymmetric counter-flow.

As a final demonstration of the general validity of this quantification of the influence of stretch rate upon the turbulent burning velocity, the best curves of u_{to}/u_l in figures 12 and 14 plotted against u'_k/u_l were used in association with (42) to generate values of u_t/u_l from the values of A_r, for each value of u'_k/u_l, given by the stretch rate PDF and $\mathscr{K}_{qt}Le$. This procedure was followed first for the integrated PDF given by (38)–(41) and $a = 0.0132$ and for the asymmetric counterflow against burnt products condition for $\mathscr{K}_{qt}Le$, given by the full line curve in figure 9. For the best curve of u_{to}/u_l in figure 12, the results are shown by the broken curves in figure 16, while the full line curves are experimental. The procedure next was followed with the best curve of u_{to}/u_l in figure 14, the same PDF, but the value of $\mathscr{K}_{qt}Le$ given by (43), with the results shown by the broken curves in figure 17. These are closer to the experimental values of u_t/u_l than are the broken curves of figure 16. This optimization suggests (43) gives an appropriate value of $\mathscr{K}_{qt}Le$, in combination with (22), (27) and (28) with $a = 0.0132$ for the PDF of stretch rates. Relevant integrations are given by (38)–(41).

The mode of generation of the u_t/u_l against u'_k/u_l curves at different values of KLe clearly shows the roles of u'_k in wrinkling the flame to increase the burning

velocity and of flame stretch in reducing it. With regard to the latter, the magnitude of the burning velocity is governed by the proportion of the mean flame front area that is quenched.

6. Discussion

Despite uncertainties in the flame stretch rate distribution and the extinction stretch rate data, the present approach reveals that good agreement can be obtained between predicted and measured values of turbulent burning velocity. Furthermore, maximum generality has been achieved through the use of dimensionless groups. The stretch rate PDFs of Pope and coworkers are for rather lower values of turbulent Reynolds number than are covered by the burning velocity data and the blending of the randomly orientated flame surface and a material surface by the stretch dependency factor is arbitrary and requires further study. Nevertheless, the work of Pope provides a good basis for the selection of an appropriate PDF.

Bray (1990) has used a flamelet analysis based on the Bray–Libby–Moss (1985) model to derive an expression for the u_t/u_l ratio, which he compared with the experimental data of Abdel-Gayed *et al.* (1987). A log-normal distribution of the viscous dissipation rate was used for the stretch rate distribution and this acted on a stoichiometric laminar methane–air flame (Cant *et al.* 1991). In the course of this study, the ratio of effective laminar burning velocity to the unstretched value was derived for different values of the standard deviation of the distribution. The value of this ratio is determined by the value of K and its square root is essentially A_r. With a value of 2 for the standard deviation and of 1 for Le, values of A_r derived in this way from the work of Bray are plotted in figure 15. They suggest a somewhat greater quenching effect than appears in the present analysis.

In the course of the present work optimizations of both stretch rate PDF and extinction stretch rate data have been suggested in the light of the experimental data on u_t/u_l. Examples of this are the selections, within limits, of a suitable value for a, the stretch dependency factor, of a suitable profile of $\mathscr{K}_{qt}Le$ against KLe and a preference for asymmetric rather than symmetric laminar counterflow data. There are clear limits to this procedure and wide uncertainty bands exist for the values of all key parameters.

The degree of generalization of stretch rate extinction embodied in the use of present $\mathscr{K}_{qt}Le$ data might reasonably be valid for paraffin fuel–air mixtures, but this is not necessarily so for olefines, acetylenes, aromatics and hydrogen or oxidants other than air, although the u_t/u_l experimental data cover a variety of fuels. The assumption that negative stretch rates have no effect on the heat release rate–temperature profile also is unsubstantiated and this effect requires research. The importance of negative stretch rate is indicated by figure 10 and further theoretical and experimental researches are necessary to elucidate its role. In view of these uncertainties it might, *pro tem*, be sufficiently accurate in computations to express the turbulent extinction stretch rate by the equation of the broken curve B in figure 9, namely (43), and to use the suggested stretch rate PDF, with $a = 0.0132$.

The present findings are of importance to computations of combustion flow fields. Only when there is a well-defined mean flame front can a turbulent burning velocity express the rate of combustion. In complex flows, particularly those with recirculation, it can be more convenient to express this rate by the computed field distribution of $\tilde{q}_t$ (Bradley *et al.* 1988*a*; Bradley & Lau 1990; Abd Al-Masseeh *et al.* 1991*a*, *b*; Bradley *et al.* 1991). Here the effects of flame stretch enter through the

PHILOSOPHICAL TRANSACTIONS OF THE ROYAL SOCIETY A MATHEMATICAL, PHYSICAL & ENGINEERING SCIENCES

mathematical modelling of the turbulence in the field computation and, in particular, through the computed mean values of the specific dissipation rate of the turbulent energy, ϵ. The relationship between ϵ and the eulerian mean strain rate, u'/λ, is given by (21). In Bradley *et al.* (1991) a quasi-gaussian PDF of stretch rates was assumed and the values of s_{qt} and $\bar{s}$ led to

$$A_r = \mathrm{erf}\,(0.41Le/0.89KLe\pi^{0.5}). \tag{44}$$

The premixture was methane–air of equivalence ratio 0.84 for which $Le = 0.975$ (Abdel-Gayed *et al.* 1984) and it is informative to compare these values with those given by (38)–(41) with $\mathscr{K}\,Le$ given by (43) and $a = 0.0132$. They are identical when $KLe = 1.2$, but when $KLe = 0.21$, (44) gives a value of 0.91, while (38)–(41) give a significantly smaller value of 0.43. For $KLe = 1.9$ the respective values are 0.14 and 0.23.

The instantaneous values of turbulent energy dissipation rate are governed by appropriate PDFs and both temporal and spatial correlations. At any instant the flame can propagate only in those regions where the stretch rate is less than s_{qt}, corresponding to the shaded régime in figure 10.

This consideration leads to a wider régime of applicability of laminar flamelet modelling than is generally recognized. In terms of (21) there can only be a flame when a $\partial u/\partial x$ term is less than s_{qt}. This implies that, at that instant, for a flame to propagate, the local turbulent energy dissipation rate must not exceed an upper limit, ϵ_f. From (21)

$$\epsilon_f \leqslant 15\nu(s_{qt})^2. \tag{45}$$

It also follows from (21) and (45) that

$$\epsilon_f/\epsilon \leqslant (s_{qt}/(u'/\lambda))^2 = (\mathscr{K}_{qt}/K)^2. \tag{46}$$

A dissipative timescale $\tau_f = (\nu/\epsilon_f)^{0.5}$ can be defined for this region, analogous to the Kolmogorov timescale, $\tau_\eta = (\nu/\epsilon)^{0.5}$. Hence

$$\tau_f/\tau_\eta = (\epsilon/\epsilon_f)^{0.5} \geqslant (K/\mathscr{K}_{qt}). \tag{47}$$

The existence of both an extinction rate and a distribution of stretch rates suggests some modification to the criterion for the existence of a wrinkled laminar flame structure, given in §1 as $\tau_\eta \geqslant \delta_l/u_l$. This might be replaced by

$$\tau_f \geqslant \delta_l/u_l, \tag{48}$$

which together with the definitions of τ_η, K, and (21) and (47), yield

$$\mathscr{K}_{qt} \leqslant 0.258. \tag{49}$$

The values of $\mathscr{K}_{qt}Le$ shown by curve B in figure 9 suggest this condition usually can be fulfilled to give a wider régime of flamelet burning than the more common criterion of $K \leqslant 0.258$. This can explain the otherwise surprising result that laminar flamelet modelling has given good predictive accuracy with increasing turbulence even up to the point of complete flame blow-off (Abd Al-Masseeh *et al.* 1991*a*; Bradley *et al.* 1991).

7. Conclusions

(i) A theoretical basis has been established for correlating u_t/u_l in terms of the dimensionless group KMa, or KLe. A generalized expression for flame stretch rate enables it to be expressed in terms of appropriate velocity gradients.

(ii) A new generalization of turbulent burning velocity experimental data has been presented.

(iii) An attempt has been made, with dimensionless groups, to generalize both available laminar and turbulent flame extinction stretch rate data.

(iv) A PDF of turbulent flame stretch rates has been proposed which depends upon KLe. One of the principal uncertainties concerns the influence of negative stretch rate.

(v) The experimental data on turbulent burning velocity are well predicted by a theory based on flamelet extinction by flame stretch with the proposed generalized stretch rate PDF and extinction stretch rate data.

(vi) An explanation is offered as to why a laminar flamelet modelling of complex combusting flows appears to have a wider range of validity than is generally supposed.

The authors thank the Commission of the European Communities and the Science and Engineering Research Council for support.

References

Abd Al-Masseeh, W. A., Bradley, D., Gaskell, P. H., Ishikawa, A. & Lau, A. K. C. 1991 *a* The rotating matrix swirling gas burner: performance and computational design. Eurotech Direct '91, C413/043. London: Institution of Mechanical Engineers.

Abd Al-Masseeh, W. A., Bradley, D., Gaskell, P. H. & Lau, A. K. C. 1991 *b* Turbulent premixed swirling combustion: direct stress, strained flamelet modelling and experimental investigation. In *23rd Int. Symp. on Combustion*, pp. 825–833. Pittsburgh: The Combustion Institute.

Abdalla, A. Y., Bradley, D., Chin, S. B. & Lam, C. 1982 Temperature fluctuations in a jet-stirred reactor and modelling implications. In *19th Int. Symp. on Combustion*, pp. 495–502. Pittsburgh: The Combustion Institute.

Abdel-Gayed, R. G., Al-Khishali, K. J. & Bradley, D. 1984 Turbulent burning velocities and flame straining in explosions. *Proc. R. Soc. Lond.* A **391**, 393–414.

Abdel-Gayed, R. G. & Bradley, D. 1981 A two eddy theory of premixed turbulent flame propagation. *Phil. Trans. R. Soc. Lond.* A **301**, 1–25.

Abdel-Gayed, R. G. & Bradley, D. 1982 The influence of turbulence upon the rate of turbulent burning. *Fuel-air explosions* (ed. J. H. S. Lee & C. M. Guirao). Montreal: University of Waterloo Press.

Abdel-Gayed, R. G. & Bradley, D. 1985 Criteria for turbulent propagation limits of premixed flames. *Combust. Flame* **62**, 61–68.

Abdel-Gayed, R. G., Bradley, D., Hamid, M. N. & Lawes, M. 1985 Lewis number effects on turbulent burning velocity. In *20th Int. Symp. on Combustion*, pp. 505–512. Pittsburgh: The Combustion Institute.

Abdel-Gayed, R. G., Bradley, D. & Lawes, M. 1987 Turbulent burning velocities: a general correlation in terms of straining rates. *Proc. R. Soc. Lond.* A **414**, 389–413.

Abdel-Gayed, R. G., Bradley, D. & Lau, A. K. C. 1989 *a* The straining of premixed turbulent flames. In *22nd Int. Symp. on Combustion*, pp. 731–738. Pittsburgh: The Combustion Institute.

Abdel-Gayed, R. G., Bradley, D., Lawes, M. & Lung, F. K.-K. 1988 Premixed turbulent burning during the early stages of an explosion. In *21st Int. Symp. on Combustion*, pp. 497–504. Pittsburgh: The Combustion Institute.

Abdel-Gayed, R. G., Bradley, D. & Lung, F. K.-K. 1989 *b* Combustion regimes and the straining of turbulent premixed flames. *Combust. Flame* **76**, 213–218.

Andrews, G. E. & Bradley, D. 1972 The burning velocity of methane–air mixtures. *Combust. Flame* **19**, 275–288.

Andrews, G. E., Bradley, D. & Lwakabamba, S. B. 1975 Turbulence and turbulent flame propagation: a critical appraisal. *Combust. Flame* **24**, 285–304.

Ballal, D. R. 1979 The influence of laminar burning velocity on the structure and propagation of turbulent flames. *Proc. R. Soc. Lond.* A **367**, 485–502.

Ballal, D. R. & Lefebvre, A. H. 1975 The structure and propagation of turbulent flames. *Proc. R. Soc. Lond.* A **344**, 217–234.

Batchelor, G. K. 1952 The effect of homogeneous turbulence on material lines and surfaces. *Proc. R. Soc. Lond.* A **213**, 349–366.

Batchelor, G. K. 1967 *An introduction to fluid dynamics.* New York: Cambridge University Press.

Becker, H., Arnold, A., Suntz, R., Monkhouse, P., Wolfrum, J., Maly, R. & Pfister, W. 1990 Investigation of flame structure and burning behaviour in an IC engine simulator by 2D-LIF of OH radicals. *Appl. Phys.* B **50**, 473–478.

Bilger, R. W. 1989 The structure of turbulent nonpremixed flames. In *22nd Int. Symp. on Combustion*, pp. 475–488. Pittsburgh: The Combustion Institute.

Bollinger, L. M. & Williams, D. T. 1949 *Tech. Notes Natn. Advis. Comm. Aeronaut., Wash.* Rep. no. 1707:

Borghi, R. 1985 In *Recent advances in the aerospace sciences* (ed. C. Bruno & C. Casci), pp. 117–138. New York: Plenum Press.

Bradley, D., Chen, Z. & Swithenbank, J. R. 1989*a* Burning rates in turbulent fine dust–air explosions. In *22nd Int. Symp. on Combustion*, pp. 1767–1775. Pittsburgh: The Combustion Institute.

Bradley, D., Chin, S. B., Gaskell, P. H., Lau, A. K. C. & Missaghi, M. 1987 Mathematical modelling of turbulent combustion. *Int. Conf. on Combustion in Engine Technology*, pp. 315–324. London: Institution of Mechanical Engineers.

Bradley, D., Chin, S. B., Kwa, L. K., Lau, A. K. C. & Missaghi, M. 1988*a* Laminar flamelet modelling of recirculating premixed methane and propane–air combustion. *Combust. Flame* **71**, 109–122.

Bradley, D., Hynes, J., Lawes, M. & Sheppard, C. G. W. 1988*b* Limitations to turbulence-enhanced burning rates in lean burn engines. *Int. Conf. on Combustion in Engines – Technology and Applications*, pp. 17–24. London: Institution of Mechanical Engineers.

Bradley, D., Gaskell, P. H. & Lau, A. K. C. 1991 A mixedness–reactedness flamelet model for turbulent diffusion flames. In *23rd Int. Symp. on Combustion*, pp. 685–692. Pittsburgh: The Combustion Institute.

Bradley, D. & Lau, A. K. C. 1990 The mathematical modelling of premixed turbulent combustion. *Appl. Chem.* **62**, 803–814.

Bradley, D., Lau, A. K. C. & Missaghi, M. 1989*b* Response of compensated thermocouples to fluctuating temperatures: computer simulation, experimental results and mathematical modelling. *Combust. Sci. Technol.* **64**, 119–134.

Bray, K. N. C. 1990 Studies of the turbulent burning velocity. *Proc. R. Soc. Lond.* A **431**, 315–335.

Bray, K. N. C., Libby, P. A. & Moss, J. B. 1985 Unified modeling approach for premixed turbulent combustion – Part 1: general formulation. *Combust. Flame* **61**, 87–102.

Bray, K. N. C., Champion, M. & Libby, P. A. 1988 The correlation functions for flamelet crossings in premixed turbulent flames. *Combust. Sci. Technol.* **59**, 463–469.

Bray, K. N. C., Champion, M. & Libby, P. A. 1989 Mean reaction rates in premixed turbulent flames. In *22nd Int. Symp. on Combustion*, pp. 763–769. Pittsburgh: The Combustion Institute.

Cant, R. S., Pope, S. B. & Bray, K. N. C. 1991 Modelling of flamelet surface-to-volume ratio in turbulent premixed combustion. In *23rd Int. Symp. on Combustion*, pp. 809–815. Pittsburgh: The Combustion Institute.

Clavin, P. 1985 Dynamic behavior of premixed flame fronts in laminar and turbulent flows. *Prog. Energy Combust. Sci.* **11**, 1–59.

Clavin, P. 1988 Theory of flames. In *Disorder and mixing* (ed. Guyon *et al.*). NATO ASI, Ser. E **152**, pp. 293–315. Kluwer Academic Publishers.

Clavin, P. & Joulin, G. 1983 Premixed flames in large scale and high intensity turbulent flow. *J. Phys. Lett.* **44**, L-1.

Clavin, P. & Williams, F. A. 1979 Theory of premixed-flame propagation in large-scale turbulence. *J. Fluid Mech.* **90**, 589–604.

PHILOSOPHICAL TRANSACTIONS OF THE ROYAL SOCIETY A MATHEMATICAL, PHYSICAL & ENGINEERING SCIENCES

Clavin, P. & Williams, F. A. 1981 Effects of Lewis number on propagation of wrinkled flames in turbulent flow. In *Combust. Reactive Systems Prog. Aeronautics Astronautics* **76**, 403–411.

Clavin, P. & Williams, F. A. 1982 Effects of molecular diffusion and of thermal expansion on the structure and dynamics of premixed flames in turbulent flows of large scale and low intensity. *J. Fluid Mech.* **116**, 251–282.

Damköhler, G. 1940 Der einfluss der turbulenz auf die flammengesch windigkeit in gasgemischen. *Z. F. Elektrochem.* **46**, 601–652.

Dandeker, K. V. & Gouldin, F. C. 1982 Temperature and velocity measurements in premixed turbulent flames. *AIAA Jl* **20**, 652–659.

Dixon-Lewis, G. 1988*a* Numerical modelling of strained flames with complex chemistry. In *Proc. Workshop on Gas Flame Structure: Part 2*, pp. 3–37. Novosibirsk: USSR Academy of Sciences (Siberian Division).

Dixon-Lewis, G. 1988*b* Structure and extinction of strained premixed flames. *Dynamics of reactive systems. Part 1. Flames. Prog. Astronautics Aeronautics* **113**, 166–183. Washington: AIAA.

Dixon-Lewis, G. & Islam, S. M. 1982 Flame modelling and burning velocity measurement. In *19th Int. Symp. on Combustion*, pp. 283–291. Pittsburgh: The Combustion Institute.

Grover, J. H., Fales, E. N. & Scurlock, A. C. 1963 Turbulent flame studies in two-dimensional open burners. In *9th Int. Symp. on Combustion*, pp. 21–35. New York: Academic Press.

Hamamoto, Y., Ohkawa, H., Yamamoto, H. & Sugahara, R. 1984 Effects of turbulence on combustion of homogeneous mixture of fuel and air. *Bull. JSME* **27**, 756–762.

Harper, C. M. 1989 Turbulence and combustion instabilities in engines. Ph.D. thesis, University of Leeds.

Hinze, J. O. 1975 *Turbulence*. New York: McGraw-Hill.

Karlovitz, B. 1954 *AGARD*, pp. 247–262. London: Butterworths.

Karlovitz, B., Denniston, D. W. & Wells, F. E. 1951 Investigation of turbulent flames. *J. chem. Phys.* **19**, 541–547.

Karpov, V. P., Semenov, E. S. & Sokolik, A. S. 1959 *Dokl. Akad. Nauk SSSR* **128**, 1220–1222.

Kee, R. J., Miller, J. A. & Evans, G. H. 1988 A computational model of the structure and extinction of strained, opposed flow, premixed methane–air flames. In *21st Int Symp. on Combustion*, pp. 1479–1494. Pittsburgh: The Combustion Institute.

Khramtsov, V. A. 1959 Investigation of pressure effect on the parameters of turbulence and on turbulent burning. In *7th Int. Symp. on Combustion*, pp. 609–614. London: Butterworths.

Kido, H., Wakuri, Y. & Nakashima, K. 1983 *ASME/JSME Thermal Engng Joint Conference*, vol. 4, pp. 183–190.

Klimov, A. M. 1983 Premixed turbulent flames – interplay of hydrodynamic and chemical phenomena. *AIAA Prog. Astronautics Aeronautics* **88**, 133–146.

Kozachenko, L. S. 1960*a* The combustion of gasoline air mixtures in turbulent flow. In *3rd All-Union Congress on Combustion Theory, Moscow* **1**, 126–137.

Kozachenko, L. S. 1960*b* *Bull. Acad. Sci. USSR, Div. Chem. Sci.* **1**, 37–44.

Kozachenko, L. S. & Kuznetsov, I. L. 1965 Burning velocity in a turbulent stream of a homogeneous mixture. *Combust. explos. shock waves* **1**, 22–30.

Law, C. K., Zhu, D. L. & Yu, G. 1988 Propagation and extinction of stretched premixed flames. In *21st Int. Symp. on Combustion*, pp. 1419–1426. Pittsburgh: The Combustion Institute.

Lawes, M. 1991 The refurbishment and commissioning of the SERC CARS equipment and an assessment of its value in combustion research. Final Report. Rep. no. T102, Department of Mechanical Engineering, University of Leeds.

Lewis, K. J. & Moss, J. B. 1979 Time-resolved scalar measurements in a confined turbulent premixed flame. In *17th Int. Symp. on Combustion*, pp. 267–277. Pittsburgh: The Combustion Institute.

Libby, P. A., Bray, K. N. C. & Moss, J. B. 1979 Effects of finite reaction rate and molecular transport in premixed turbulent combustion. *Combust. Flame* **34**, 285–301.

Metghalchi, M. & Keck, J. C. 1982 Burning velocities of mixtures of air with methanol, isooctane, and indolene at high pressure and temperature. *Combust. Flame* **48**, 191–210.

PHILOSOPHICAL TRANSACTIONS OF THE ROYAL SOCIETY A MATHEMATICAL, PHYSICAL & ENGINEERING SCIENCES

Markstein, G. H. 1951 Experimental and theoretical studies of flame front stability. *J. Aerospace Sci.* **18**, 199–209.

Markstein, G H. 1964 *Nonsteady flame propagation*. Oxford: Pergamon Press.

Peters, N. 1988 Laminar flamelet concepts in turbulent combustion. In *21st Int. Symp. on Combustion*, pp. 1231–1250. Pittsburgh: The Combustion Institute.

Petrov, E. A. & Talantov, A. V. 1959 *Izv. vyssh. ucheb. Zaved., Aviat. Teknol.* **3**, 91–100.

Pope, S. B. 1989 Comment. In *22nd Int. Symp. on Combustion*, p. 738. Pittsburgh: The Combustion Institute.

Searby, G. & Quinard, J. 1990 Direct and indirect measurements of Markstein numbers of premixed flames. *Combust. Flame* **82**, 298–311.

Singh, V. P. 1975 A study of turbulent flames stabilized in a high velocity, high-temperature flow. *Combust. Sci. Technol.* **11**, 181–196.

Sivashinsky, G. I. 1990 On the intrinsic dynamics of premixed flames. *Phil. Trans. R. Soc. Lond.* A **332**, 135–148.

Smith, K. O. & Gouldin, F. C. 1978 Experimental investigation of flow turbulence effects of premixed methane–air flames. *Prog. Astronaut. Aeronaut.* **58**, 37–54.

Sokolik, A. S., Karpov, V. P. & Semenov, E. S. 1967 Turbulent combustion of gases. *Combust. explos. shock Waves* **3**, 36–45.

Stahl, G., Rogg, B. & Warnatz, J. 1988 Dynamics of reactive systems. Part 1. Flames. *Prog. Astronaut. Aeronaut.* **113**, 195. Washington: AIAA.

Stahl, G. & Warnatz, J. 1991 Numerical investigation of time-dependent properties and extinction of strained methane– and propane–air flamelets. *Combust. Flame* **85**, 285–299.

Taylor, G. I. 1935 Statistical theory of turbulence. *Proc. R. Soc. Lond.* A **151**, 421–444.

Tsuji, H. & Yamaoka, I. 1981 An experimental study of extinction of near-limit flames in a stagnation flow. In *First Specialist Meeting (Int.) of the Combustion Institute*, pp. 111–116. The Combustion Institute.

Vinckier, J. & Van Tiggelen, A. 1968 Structure and burning velocity of turbulent premixed flames. *Combust. Flame* **12**, 561–568.

Wagner, P. 1955 Burning velocities of various premixed turbulent propane flames on open burners. *Tech. Notes Natn. Advis. Comm., Wash.* no. 3575.

Williams, F. A. 1976 Criteria for existence of wrinkled laminar flame structure of turbulent premixed flames. *Combust. Flame* **26**, 269–270.

Williams, F. A. 1985 *Combustion theory*, 2nd edn. Menlo Park, California: Benjamin Cummings.

Williams G. C., Hottel, H. C. & Scurlock, A. C. 1949 Flame stabilization and propagation in high velocity gas streams. In *3rd Symp. on Combustion flame and explosion phenomena*, pp. 21–40. Baltimore: Williams and Wilkins.

Wohl, K. & Shore, L. 1955 Experiments with butane–air and methane–air flames. *Ind. Engng Chem.* **47**, 828–834.

Yeung, P. K., Girimaji, S. S. & Pope, S. B. 1990 Straining and scalar dissipation on material surfaces in turbulence: implications for flamelets. *Combust. Flame* **79**, 340–365.

Zotin, V. K. & Talantov, A. V. 1966 Influence of initial temperature on the propagation velocity of a flame in a turbulent flow of a homogeneous mixture. *Izv. vyssh. ucheb. Zaved., Aviat. Teknol.* **1**, 115–122.

Received 3 May 1991; accepted 24 July 1991

PHILOSOPHICAL TRANSACTIONS OF THE ROYAL SOCIETY A MATHEMATICAL, PHYSICAL & ENGINEERING SCIENCES